Progress In Electromagnetics Research B, Vol. 58, 167–180, 2014

Geometrical and Physical Parameters Affecting Distant Electric Fields Radiated by Lightning Return Strokes

Carlo Petrarca*

Abstract—In this paper detailed numerical results are presented for the estimation of the electric field generated by the first return stroke, in order to reproduce the main characteristics of field waveforms measured at distances beyond 50 km. The effect of parameters such as the lightning channel geometry, distance from the source, return-stroke current speed, its attenuation along the channel is discussed by comparing numerical and experimental results.

1. INTRODUCTION

Lightning protection is a critical aspect for the safety of people and security and economics of power systems. Direct lightning strikes can cause considerable damage, given the extremely high peak values of current they carry, maximum rate of change of current, amount of transferred charge, and time integral of the Joule heating power [1].

Serious damages may also be due to indirect lightning strokes, that is by lightning flashes to ground in proximity of power systems and components, especially if we consider that modern apparatuses are characterized by the presence of ever increasing control and processing electronics that may be severely damaged by the indirect effects of lightning [2].

In order to design an effective lightning protection system of buildings and power electric systems and to properly dimension electrical components, it is therefore necessary to estimate electric and magnetic fields generated by lightning channels [3] which can be used as input to electromagnetic models for the calculation of induced voltages and currents and the prediction of their propagation along distribution lines or inside components [4–6].

In particular, a reliable model should be able to reproduce the main features of electric and magnetic fields generated at close and far distance by return stroke flashes, which are the most powerful known lightning processes [7, 8]. It should also be able to estimate the influence on fields of physical parameters like the shape of the lightning channel, the return stroke current waveform, its speed, attenuation, distortion, etc..

Electric field waveforms measured at distances ranging from 1 to 200 km from natural lightning return stroke show the following characteristics [9]:

1) flattening of vertical field at tens to hundreds of meters within 15 μs or so of the beginning of return stroke;
2) sharp initial peak at a few kilometers and beyond;
3) slow ramp following the initial peak within few tens of kilometers;
4) zero-crossing measured at 50–200 km.

Received 20 January 2014, Accepted 11 February 2014, Scheduled 16 February 2014

* Corresponding author: Carlo Petrarca (petrarca@unina.it).
The author is with the Department of Electrical Engineering and Information Technology, University of Naples Federico II, Naples 80125, Italy.

In particular, lightning return stroke fields measured at distances of about 50 km and beyond show typical waveforms characterized by a polarity inversion with a zero crossing occurring in the tens of microseconds range.

Shoory et al. [10, 11], based on modeling, focused their work on the zero-crossing time and suggested that in far-field waveforms this parameter is influenced by three main mechanisms: the duration of the return-stroke current waveform, the current attenuation along the channel, and the return-stroke speed. They showed that the higher the attenuation of the current along the channel, the earlier the polarity reversal of the field and that higher propagation speeds correspond to earlier polarity reversal times. Moreover, they identified two engineering models, the modified transmission line linear (MTLL) and the modified transmission line exponential (MTLE), as able to reproduce the typical zero-crossing times.

The aim of the present paper is to deeply investigate distant electric field by taking into account not only the zero-crossing times, but also the shape and magnitude of the entire field waveforms. Different influencing factors will be considered, namely the return stroke speed, the distance from the lightning source and, last but not least, the channel geometry, in order to reproduce the measured fields and try to explain the differences between the fields generated by first return strokes. Vertical and non-vertical lightning channels will be taken into account [12, 13] and three engineering models, the transmission line (TL) and the two models derived from it and identified by Shoory et al. [10], the MTLL and the MTLE, will be employed in order to reproduce the entire electric field waveform. Numerical results will also be compared to experimental data [14, 15].

The paper is organized as follows. After the present introduction, in Section 2 the main characteristics of distant electric field waveforms are described; in Section 3 the adopted model of tortuous lightning path is reviewed together with the electric field calculation; Section 4 is devoted to the presentation and discussion of numerical results; in the last section the concluding remarks are given.

2. CHARACTERISTICS OF DISTANT ELECTRIC FIELDS

The main features of distant electric field waveshapes are summarized in Figure 1 [14]. At distances greater than 100 km they tend to be oscillatory, showing two cycles. They include a sharp initial peak E_p, a zero-to peak risetime T_R, a zero-crossing time T_1, an opposite polarity overshoot (OPO) E_{OS}, an OPO duration T_2, with E_{ref} being the reference (background) field. The second positive half-cycle has been interpreted as ionospheric reflection [15] and will not be considered in the following.

The features mentioned above are generally used as a benchmark in order to check the ability of return stroke models to reproduce distant fields. In most of the previous model-validation studies, primarily zero-crossing time was used to characterize the distant fields waveforms.

According to Haddad and Rakov [15, 16], the overwhelming majority of both first and subsequent stroke field waveforms at 50 to 350 km (96 and 88%, respectively) exhibit opposite polarity overshoots, while subsequent stroke signatures at 50 to 100 km are appreciably less likely (72% vs. 89%) to be bipolar than their first-stroke counterparts. The results, substantially, confirm the data of first return

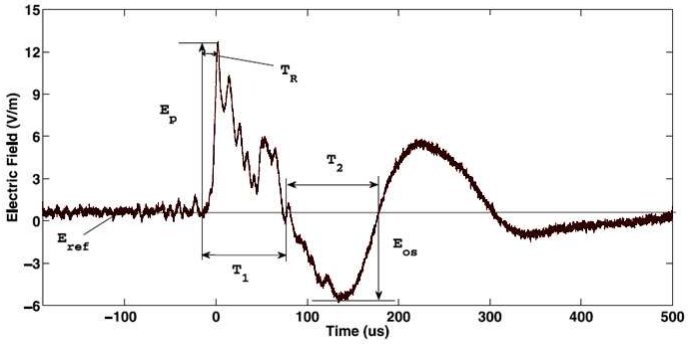

Figure 1. Electric field waveform characteristics (from [14]).

strokes collected by Pavlick et al. [14], who found that about 4% of electric field waveforms measured in the range from 50 to 250 km did not exhibit a pronounced zero-crossing within 400 µs of the initial peak.

As shown in Table 1, the arithmetic mean of zero crossing times T_1 measured in [15] is 89 µs for first strokes and 68 µs for subsequent strokes; the value for first return stroke is sensibly higher than that reported in [14] ($T_1 = 53$ µs) which suffers from bandwidth restrictions of the measuring instrumentation.

Table 1. Characteristics of distant electric fields.

	First stroke			Subsequent strokes		
	T_1 [µs]	T_2 [µs]	E_p/E_{os}	T_1 [µs]	T_2 [µs]	E_p/E_{os}
Pavlick [14]	53	90	5.4	/	/	/
Haddad [15]	89	107	3.5	68	86	5.4

The measured ratio E_p/E_{os} of initial peak to Opposite Polarity Overshoot is 3.5 at distances greater than 50 km in [15] and is equal to 5.4 in [14]. For subsequent strokes the value reported in [15] is equal to 5.4. The ratio is strongly influenced by distance and decreases to 2 in the 250–300 km range; moreover, it is higher for subsequent strokes ($E_p/E_{os} = 5.4$). The values of the *OPO* duration T_2 for first strokes are larger than T_1 both in [15] ($T_2 = 107$ µs) and in [14] ($T_2 = 90$ µs).

What are the factors affecting such parameters? Which is their influence? In Section 4 an analysis of numerically calculated electric fields will be carried out in order to obtain a relation between the lightning channel geometry, the computed fields and the measured fields.

3. COMPUTATION OF EM FIELDS RADIATED BY NON VERTICAL LIGHTNING CHANNELS

3.1. Calculation of Electric Field

The adopted engineering lightning return stroke model is fully described in [12, 17], in which the lightning channel is not vertical and a closed-form solution for the electric and magnetic fields generated by a channel of arbitrary location and slope is given. In the following only the final expression of electric fields will be given.

The model is able to justify the fine structure of the fields produced by cloud-to-ground discharges in both natural and triggered lightning. For instance, recently, it was shown that at close distances the effect of the inclination of the lower segments in the channel strongly alters the amplitude of the electric field while, at distances in the order of some km, the tortuosity of the lightning path modifies the jaggedness of the time waveform of the fields [18].

It is possible to calculate analytically the step response of an arbitrarily oriented channel **C** by assuming that it is traversed by a unit step function current

$$i\left(z',t\right) = \left\{u\left(t - \frac{z'}{v}\right)\left[u\left(z'\right) - u\left(z' - h\right)\right]\right\} \tag{1}$$

where v is the return stroke front speed and u the Heaviside step function.

If the channel is composed of N segments, the overall effect of the tortuous channel can then be found by summing up all its individual components.

Once the electric field due to a unit step current has been calculated, by adopting a suitable convolution summation, the field $y(t)$ associated with an arbitrary current waveform $i(t)$ can then be obtained using Duhamel's theorem [19]

$$y(t) = \int_0^t \frac{di\left(\tau\right)}{d\tau} s\left(t - \tau\right) d\tau \tag{2}$$

By adopting a proper cylindrical reference system $\Re$ (Figure 2), with the z-axis coincident with the axis of the channel segment and the origin coincident with the starting point **O**, the mathematical

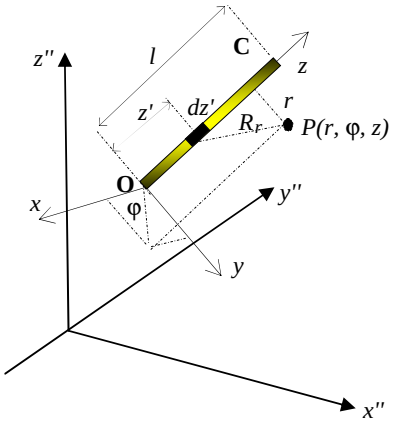

Figure 2. Generic discharge channel **C** and main geometrical parameters.

expression of the fields can be simplified since only the r and the z components of the electric field are present:

The generated electric field in the cylindrical reference system $\Re$ at the observation point $P(r,\, \varphi,\, z)$ assume the formulation reported in (3).

$$\begin{cases} E_r = \dfrac{r\left[-tu\left(t-\frac{\sqrt{r^2+z^2}}{c}\right)\right]}{4\pi\varepsilon_0\left(\sqrt{r^2+z^2}\right)^3} + \dfrac{r\left[\left(t-\frac{l}{v}\right)u\left(t-\frac{l}{v}-\frac{\sqrt{r^2+(z-l)^2}}{c}\right)\right]}{4\pi\varepsilon_0\left(\sqrt{r^2+(z-l)^2}\right)^3} + \int\limits_0^l g\,(t)dz' \\ E_\varphi = 0 \\ E_z = \dfrac{z\left[-tu\left(t-\frac{\sqrt{r^2+z^2}}{c}\right)\right]}{4\pi\varepsilon_0\left(\sqrt{r^2+z^2}\right)^3} + \dfrac{(z-l)\left[\left(t-\frac{l}{v}\right)u\left(t-\frac{l}{v}-\frac{\sqrt{r^2+(z-l)^2}}{c}\right)\right]}{4\pi\varepsilon_0\left(\sqrt{r^2+(z-l)^2}\right)^3} + \int\limits_0^l p\,(t)\,dz' \end{cases} \tag{3}$$

where c is the speed of light, and the integrals $\int\limits_0^l g(t)dz'$ and $\int\limits_0^l p(t)dz'$ have the following values:

$$\int\limits_0^l g\,(t)\,dz' = \begin{cases} 0 & \text{if } z_0\,(t) < 0 \\ \dfrac{1}{4\pi\varepsilon_0 v}\left[\dfrac{\sin\,(\varphi_2)-\sin\,(\varphi_1)}{r} + \dfrac{r}{cR_0^2\left|-\frac{1}{v}-\frac{(z_0(t)-z)}{cR_0}\right|}\right] & \text{if } 0 \le z_0\,(t) \le l \\ \dfrac{1}{4\pi\varepsilon_0 v}\left[\dfrac{\sin\left(\text{arctg}\left(\frac{l-z}{r}\right)\right)-\sin\left(\text{arctg}\left(\frac{-z}{r}\right)\right)}{r}\right] & \text{if } z_0\,(t) > l \end{cases} \tag{4}$$

$$\int\limits_0^l p\,(t)\,dz' = \begin{cases} 0 & \text{if } z_0\,(t) < 0 \\ \dfrac{1}{4\pi\varepsilon_0 v}\left[\dfrac{\cos\,(\varphi_2)-\cos\,(\varphi_1)}{r} + \dfrac{(z-z_0\,(t))}{cR_0^2\left|-\frac{1}{v}-\frac{(z_0(t)-z)}{cR_0}\right|}\right] & \text{if } 0 \le z_0\,(t) \le l \\ \dfrac{1}{4\pi\varepsilon_0 v}\left[\dfrac{\cos\left(\text{arctg}\left(\frac{l-z}{r}\right)\right)-\cos\left(\text{arctg}\left(\frac{-z}{r}\right)\right)}{r}\right] & \text{if } z_0\,(t) > l \end{cases} \tag{5}$$

in which

$$z_0\,(t) = \frac{\frac{t}{v}-\frac{z}{c^2}-\sqrt{\left(\frac{t}{v}-\frac{z}{c^2}\right)^2-\left(\frac{1}{v^2}-\frac{1}{c^2}\right)\left(t^2-\frac{r^2}{c^2}-\frac{z^2}{c^2}\right)}}{\left(\frac{1}{v^2}-\frac{1}{c^2}\right)} \tag{6}$$

and

$$\begin{cases} \varphi_2 = \text{arctg}\left(\dfrac{z_0\,(t) - z}{r}\right) \\ \varphi_1 = \text{arctg}\left(\dfrac{-z}{r}\right) \\ R_0 = \sqrt{r^2 + (z - z_0\,(t))^2} \end{cases} \tag{7}$$

Since a perfectly conducting plane is considered, the method of the images can be applied, and the contribution of the image sources can be obtained in the same manner by adopting a cylindrical co-ordinate system with the z-axis coincident with the axis of the image channel.

The channel base current adopted in the simulations is shown in Figure 3 and has the following expression [20]:

$$i(0,t) = \frac{I_0}{\eta}\frac{(t/\tau_1)^n}{1+(t/\tau_1)^n}\exp\left(-t/\tau_2\right) \tag{8}$$

with

$$\eta = \exp\left[-(\tau_1/\tau_2)(n\tau_2/\tau_1)^{(1/n)}\right] \tag{9}$$

The values of its parameters are in Table 2.

Table 2. Parameters of channel base current.

	I_0 [kA]	τ_1 [µs]	τ_2 [µs]	n
First return stroke	28	1.8	95	2

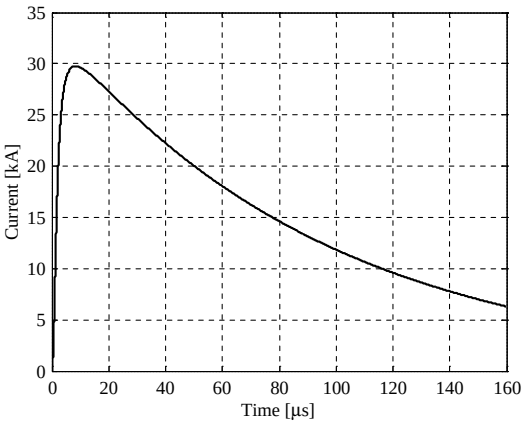

Figure 3. Channel base current waveform.

The current is assumed to propagate at constant speed v and decay with height according to three different models:

a) Transmission Line (TL) return stroke model, in which the current $i(0,\,t)$ specified at the base of the channel is assumed to propagate upward at a constant speed v as if the channel were an ideal transmission line [21].

$$i\,(z,t) = i\left(0, t - \frac{z}{v}\right) \tag{10}$$

b) Modified Transmission Line Linear model (MTLL) which considers a linear current decay along the channel, from a maximum at the channel base ($z = 0$) to zero at the channel top ($z = H$) [22].

$$i\,(z,t) = i\left(0, t - \frac{z}{v}\right)\left(1 - \frac{z}{H}\right) \tag{11}$$

The parameter H (reference height of channel) has been chosen equal to 7.5 km above ground level.

c) Modified Transmission Line Exponential model (MTLE) in which the decrease of current amplitude along the channel is assumed to be exponential according to the constant λ, chosen equal to 2000 m [23]. In this hypothesis the current at the channel top is not zero.

$$i\left(z,t\right)=i\left(0,t-\frac{z}{v}\right)\cdot\exp\left(-\frac{z}{\lambda}\right) \tag{12}$$

It is important to remark that the TL model has been chosen only for its historical value, since MTLL and MTLE derive from it, while other engineering return stroke models, i.e., the Bruce-Golde (BG) [24], the Travelling Current Source (TCS) [25] and the Diendorfer-Uman [26], were not considered in the present paper since it has been analytically shown that they are not able to reproduce one of the main features of distant electric fields, that is the experimental zero crossing times T_1 [10].

4. COMPUTATIONAL RESULTS AND DISCUSSION

Electric fields were calculated at ground surface ($z=0$) at various distances d (75 km, 125 km, 275 km) from the channel base. Different channel geometries were selected (Figure 4): a) vertical channel (vc); b) inclined channel (ic); c) slanted segment channel with 8 segments (sc_8).

In particular, in the case of channels i_c and sl_8, for each distance, 4 observation points P at different azimuths were selected ($\phi=0°$, $\phi=90°$, $\phi=180°$, $\phi=270°$) in order to show the dependence of the fields on the relative position between the channel and the observer.

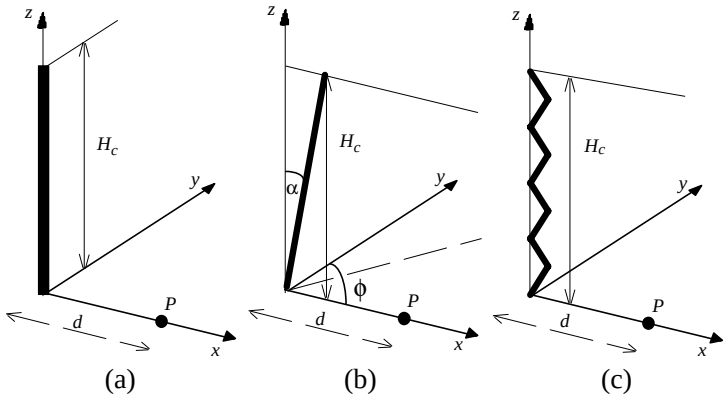

Figure 4. Channel geometries adopted in the simulations. (a) Vertical channel. (b) Inclined channel. (c) Slanted channel with 8 segments.

4.1. Effect of Propagation Model

The first analysis of the reproduced distant field has been carried out by considering the electric field produced by the first return stroke developing in a vertical channel of height $H_c=7.5$ km at the speed $v=90\,\mathrm{m/\mu s}$ ($\beta=v/c=0.3$).

As an example, in Figure 5 the field waveforms calculated at a distance $d=75$ km from the channel base, for the three propagation models, are shown. Note that in the figures the propagation delay has been removed here and thereafter, in order to show all the waveforms on the same time scale, regardless of distance.

The waveform calculated with the TL model shows the typical "image mirror effect" [27], that is the abrupt change of polarity of the electric field occurring when the current reaches the top of the channel with a non negligible amplitude. A slight discontinuity in the waveshape is also present when adopting the MTLE model since the return stroke current at the top of the channel, although small, is not equal to zero. The waveform obtained by using the MTLL model has no discontinuity since the current at the channel top is exactly zero because the reference height H has been chosen equal to the channel height H_c.

TL model is not able to reproduce the main characteristics of the fields at great distance and the waveform sensibly differs from the experimental findings; for such a reason, TL model will not be considered in the following.

On the contrary, the waveshapes of Figure 5 obtained with the MTLL and MTLE recall the typical experimental acquisitions of Figure 1 since they are characterized by well defined zero-crossing time T_1 ($T_1 = 67.9\,\mu s$ and $T_1 = 48.5\,\mu s$, respectively), Opposite Polarity Overshoot ratio ($E_p/E_{os} = 3.6$ and $E_p/E_{os} = 7.6$, respectively) and zero-to-peak risetime T_R ($T_R = 6.9\,\mu s$ and $T_2 = 5.0\,\mu s$, respectively). As concerns as the *OPO* duration T_2, it cannot be calculated since the two models do not take into account two dominant phenomena, that is the development of the in-cloud portion of the channel [1] and the ionospheric reflection [15], responsible of the second positive half-cycle of the waveforms.

The differences between the models and between experiments and simulations as a function of return stroke speed, distance from the source, and channel geometry will be discussed in the next paragraphs of Section 4.

4.2. Effect of Return Stroke Speed

A sensible effect on the radiated electric field is due to the return stroke velocity v. Figure 6 shows, for the MTLL (Figure 6(a)) and MTLE (Figure 6(b)) models, the time evolution of the electric field for

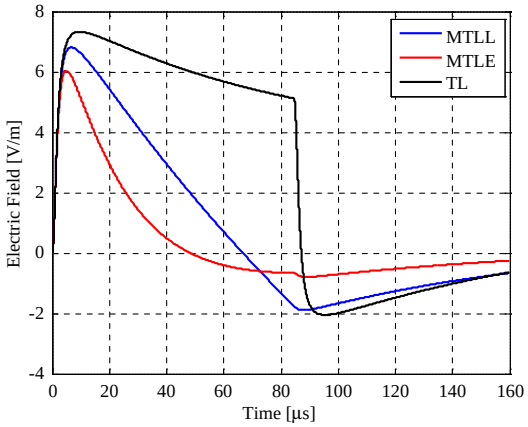

Figure 5. Electric field at ground at $d = 75\,km$ for a vertical channel (vc). Effect of propagation model.

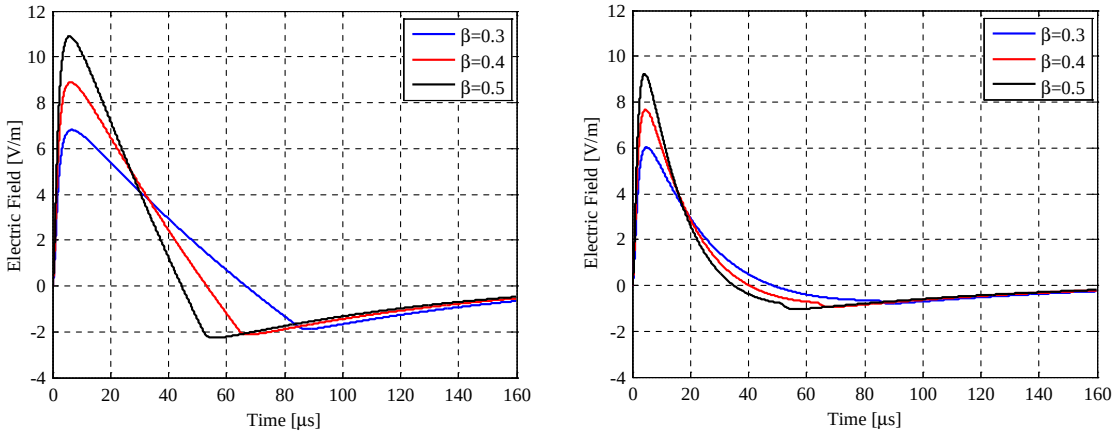

Figure 6. Electric field at ground at $d = 75\,km$ for a vertical channel (vc). MTLL (Figure 6(a)) and MTLE (Figure 6(b)). Effect of speed $v = \beta \cdot c$.

different values of the ratio $\beta = v/c$, namely $\beta = 0.3$, $\beta = 0.4$ and $\beta = 0.5$.

In both models, increasing the propagation speed results in a earlier occurrence of the zero-crossing. If we consider that the first return stroke speed is generally lower than subsequent strokes velocity [28], such results are consistent with experimental findings in which it can be deduced that zero-crossing times are longer for first return strokes compared with subsequent strokes.

An increase with speed is also observed for the ratio E_p/E_{os}, which, for instance, in the MTLL model is equal to 3.6 for $\beta = 0.3$ and becomes equal to 4.8 for $\beta = 0.5$. In the MTLE model the ratio is $E_p/E_o = 7.5$ for $\beta = 0.3$ and it increases up to $E_p/E_o = 8.7$ when $\beta = 0.5$. As concerns as the zero-to-peak risetime T_R, in both models it decreases with velocity. Also these results are consistent with experimental findings which report higher values of the ratio and smaller values of zero-to-peak risetime in the case of distant fields produced by subsequent strokes.

For a better readability, the waveform parameters calculated with simulations (both MTLL and MTLE models), together with their arithmetic mean calculated from experimental data [15], are summarized in Tables 3(a), 3(b) and 3(c) for different distances d from the channel base ($d = 75\,\text{km}$, $d = 125\,\text{km}$ and $d = 275\,\text{km}$, respectively), in the case of a vertical lightning channel. An attempt to

Table 3. (a) Calculated electric field parameters at $d = 75\,\text{km}$ as a function of β vs. measured data [15]. Vertical channel. (b) Calculated electric field parameters at $d = 125\,\text{km}$ as a function of β vs. measured data [15]. Vertical channel. (c) Calculated electric field parameters at $d = 250\,\text{km}$ as a function of β vs. measured data [15]. Vertical channel.

(a)

$d = 75\,\text{km}$				
	E_p/E_0	T_R [μs]	T_1 [μs]	T_2 [μs]
measured ($50 \div 100\,\text{km}$)	4.4	8.4	95.7	117.4
MTLL ($\beta = 0.3$)	3.6	6.9	67.9	> 80
MTLL $\beta = 0.4$)	4.2	6.4	53.2	> 110
MTLL ($\beta = 0.5$)	4.8	6.0	44.3	> 110
MTLE ($\beta = 0.3$)	7.6	5.0	48.5	> 110
MTLE ($\beta = 0.4$)	8.1	4.6	40.5	> 120
MTLE ($\beta = 0.5$)	8.8	4.3	35.0	> 120

(b)

$d = 125\,\text{km}$				
	E_p/E_0	T_R [μs]	T_1 [μs]	T_2 [μs]
measured ($100 \div 150\,\text{km}$)	3.6	9.0	96.8	131.2
MTLL ($\beta = 0.3$)	3.5	6.3	64.6	> 80
MTLL ($\beta = 0.4$)	4.0	6.2	52.0	> 100
MTLL ($\beta = 0.5$)	4.7	5.8	43.7	> 100
MTLE ($\beta = 0.3$)	6.9	4.9	46.7	> 100
MTLE ($\beta = 0.4$)	7.5	4.5	39.3	> 120
MTLE ($\beta = 0.5$)	8.3	4.1	34.1	> 120

(c)

$d = 275\,\text{km}$				
	E_p/E_0	T_R [μs]	T_1 [μs]	T_2 [μs]
measured ($250 \div 300\,\text{km}$)	2.2	8.5	78.7	104.4
MTLL ($\beta = 0.3$)	3.4	6.3	63.5	> 70
MTLL ($\beta = 0.4$)	4.0	6.1	51.3	> 110
MTLL ($\beta = 0.5$)	4.6	5.9	43.8	> 110
MTLE ($\beta = 0.3$)	6.2	4.9	46.0	> 110
MTLE ($\beta = 0.4$)	7.0	4.5	38.7	> 120
MTLE ($\beta = 0.5$)	8.3	4.2	33.8	> 120

explain the differences from simulations and experiments in the values of such parameters will be given in Section 4.4 when dealing with the effects of channel inclination.

4.3. Effect of Distance

In Figure 7 the electric field at ground, at different distances d from the channel base, is plotted vs. time both for MTLL model (Figure 7(a)) and MTLE model (Figure 7(b)) when $\beta = 0.3$.

The effect of distance can be deduced by analyzing both Figure 7 and Table 3. At distances greater than 50 km, the differences in the waveshapes at 75 km, 125 km and 275 km do not seem to be relevant as also observed in experimental tests. In fact, the decrease of zero-crossing time T_1 with distance, from 75 km to 275 km, is only about 7% for the MTLL model and 5% for the MTLE model; it is a little underestimated if compared with experimental data (about 15%).

Also the zero-to-peak risetime T_R is almost unchanged with distance; it decreases of about 8% with MTLL and of about 2% with MTLE, compared to a slight increase of about 2% calculated during experimental investigations.

The major differences from simulations and experiments can be found in the ratio E_p/E_o. Experimental results report a sensible decrease of the ratio with distance ($E_p/E_o = 4.4$ in the range 50–100 km and $E_p/E_o = 2.2$ in the range 50–100 km), while in the simulations the ratio is almost unaffected by the distance.

As described in Section 4.4 such a difference could be ascribed to the inclination of the lightning channel with respect to ground, which, at the author's knowledge, has never been investigated numerically as an influencing factor on distant electric fields.

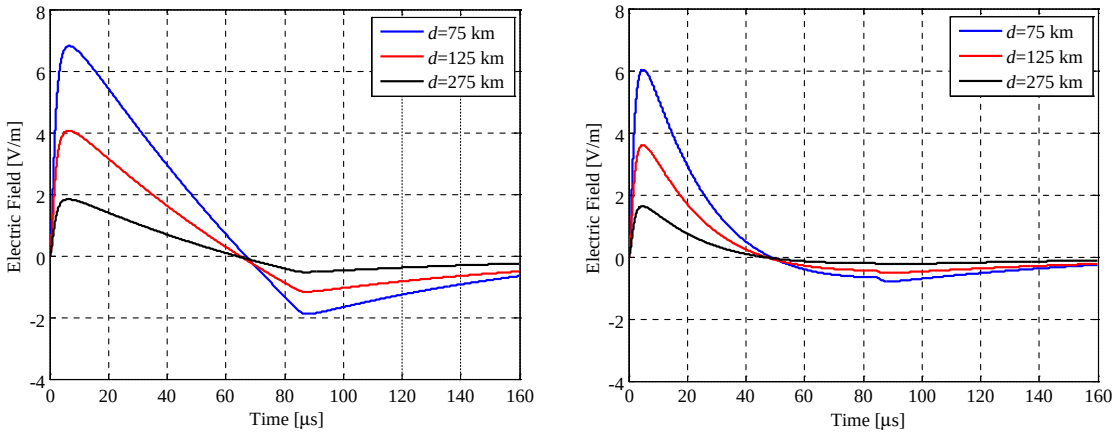

Figure 7. Electric field at ground for a vertical channel (vc) and $\beta = 0.3$, MTLL (Figure 7(a)) and MTLE (Figure 7(b)). Effect of distance d.

4.4. Effect of Channel Inclination

The lightning return stroke channel is not straight and vertical, as generally assumed in many models, but it is tortuous on scales ranging from less than 1 m to over 1 km [29]; moreover it strikes the ground at an angle less than ninety degrees with respect to the ground [30]. Lightning data are averaged to get rid of the contribution of tortuosity, and often the failure to predict fields in accordance with experimental data may be attributed to the nonvertical and nonstraight nature of the channels more than to inadequacy of the models themselves.

The simulations confirm that channel inclination is an important parameter that should be considered in testing the validity of return-stroke models and interpreting experimental data.

Typical electric field waveforms at 75 km are shown in Figure 8 for both MTLL (Figure 8(a)) and MTLE (Figure 8(b)) models; they are produced by a return stroke current flowing at $\beta = 0.3$ along an

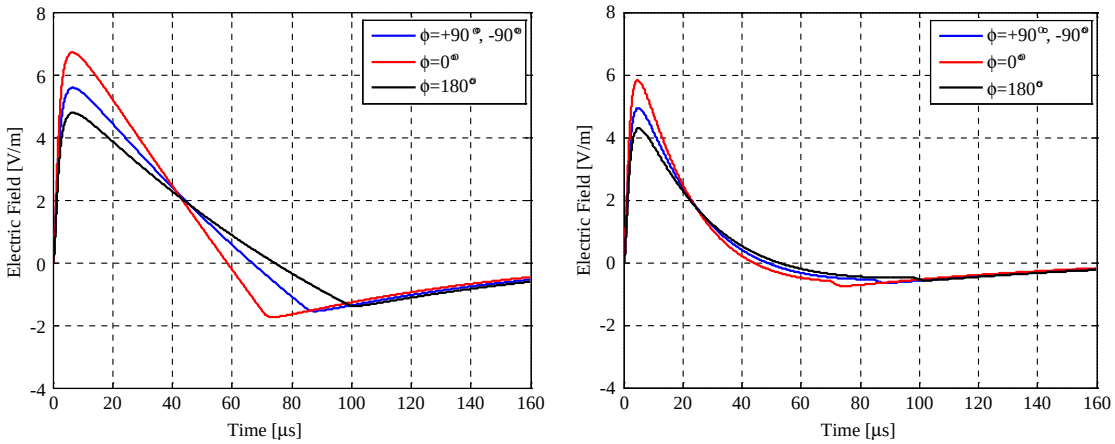

Figure 8. Electric field at ground for an inclined channel (ic) and $\beta = 0.3$, MTLL (Figure 8(a)) and MTLE (Figure 8(b)). Effect of observer position P.

Table 4. (a) Calculated electric field parameters at $d = 75$ km as a function of observation point. β=0.3. Inclined channel. (b) Calculated electric field parameters at $d = 125$ km as a function of observation point. $\beta = 0.3$. Inclined channel. (c) Calculated electric field parameters at $d = 250$ km as a function of observation point. $\beta = 0.3$. Inclined channel.

(a)

$d = 75$ km			
	E_p/E_0	T_R [μs]	T_1 [μs]
MTLL ($\phi = 0°$)	3.9	6.6	58.3
MTLL ($\phi = +90°, -90°$)	3.7	6.7	66.7
MTLL ($\phi = 180°$)	3.4	6.8	74.1
MTLE ($\phi = 0°$)	8.3	4.7	44.0
MTLE ($\phi = +90°, -90°$)	7.8	4.9	48.3
MTLE ($\phi = 180°$)	7.6	5.0	52.4

(b)

$d = 125$ km			
	E_p/E_0	T_R [μs]	T_1 [μs]
MTLL ($\phi = 0°$)	3.8	6.5	56.5
MTLL ($\phi = +90°, -90°$)	3.4	6.6	64.8
MTLL ($\phi = 180°$)	3.3	6.7	72.1
MTLE ($\phi = 0°$)	7.1	4.6	42.1
MTLE ($\phi = +90°, -90°$)	7.0	4.8	46.7
MTLE ($\phi = 180°$)	6.7	5.0	51.0

(c)

$d = 275$ km			
	E_p/E_0	T_R [μs]	T_1 [μs]
MTLL ($\phi = 0°$)	3.8	6.3	55.4
MTLL ($\phi = +90°, -90°$)	3.5	6.4	63.4
MTLL ($\phi = 180°$)	3.3	6.6	70.1
MTLE ($\phi = 0°$)	6.4	4.7	41.1
MTLE ($\phi = +90°, -90°$)	6.7	4.8	45.8
MTLE ($\phi = 180°$)	8.7	4.9	50.1

inclined lightning channel (Figure 4(b)) laying in the xz-plane with an inclination $\alpha = 35°$ with respect to the z-axis. The fields are evaluated at different azimuths ϕ in order to put in evidence the effects of the relative position of the observer with respect to the lightning path.

The results are summarized in Tables 4(a), 4(b) and 4(c), for the different observation points and distances $d = 75\,\text{km}$, $d = 125\,\text{km}$ and $d = 275\,\text{km}$, respectively. They can be compared with the data shown in Table 3 and relative to a vertical channel.

The major influence of the channel inclination can be observed in the zero-crossing time T_1 and in the ratio E_p/E_o, while the differences between a vertical and an inclined channel are almost negligible if considering the zero-to-peak risetime T_R.

Table 5. (a) E_p/E_o for channel sc_8 as a function of observation point and distance compared with the same parameter calculated for channel *vc*. ($\beta = 0.3$). (b) E_p/E_o for channel sc_8 as a function of observation point and distance compared with the same parameter calculated for channel *vc*. ($\beta = 0.4$). (c) E_p/E_o for channel sc_8 as a function of observation point and distance compared with the same parameter calculated for channel *vc*. ($\beta = 0.5$).

(a)

E_p/E_0			
	$d = 75\,\text{km}$	$d = 125\,\text{km}$	$d = 275\,\text{km}$
MTLL ($\phi = 0°$)	3.9	3.8	3.7
MTLL ($\phi = +90°, -90°$)	3.6	3.5	3.5
MTLL ($\phi = 180°$)	3.5	3.3	3.3
MTLL (*vc*)	3.6	3.5	3.4
MTLE ($\phi = 0°$)	8.1	7.4	7.1
MTLE ($\phi = +90°, -90°$)	7.6	7.0	6.8
MTLE ($\phi = 180°$)	7.1	6.5	6.5
MTLE (*vc*)	7.6	6.9	6.2

(b)

E_p/E_0			
	$d = 75\,\text{km}$	$d = 125\,\text{km}$	$d = 275\,\text{km}$
MTLL ($\phi = 0°$)	4.8	4.5	4.4
MTLL ($\phi = +90°, -90°$)	4.3	4.1	4.0
MTLL ($\phi = 180°$)	4.3	4.1	4.1
MTLL (*vc*)	4.2	4.0	4.0
MTLE ($\phi = 0°$)	8.9	8.4	8.0
MTLE ($\phi = +90°, -90°$)	8.1	7.6	7.3
MTLE ($\phi = 180°$)	7.2	7.0	6.7
MTLE (*vc*)	7.4	7.5	7.3

(c)

E_p/E_0			
	$d = 75\,\text{km}$	$d = 125\,\text{km}$	$d = 275\,\text{km}$
MTLL ($\phi = 0°$)	5.6	5.4	5.3
MTLL ($\phi = +90°, -90°$)	4.9	4.9	4.7
MTLL ($\phi = 180°$)	5.1	5.1	4.9
MTLL (*vc*)	4.8	4.7	4.6
MTLE ($\phi = 0°$)	10.0	9.3	9.0
MTLE ($\phi = +90°, -90°$)	8.9	8.3	8.0
MTLE ($\phi = 180°$)	8.0	7.5	7.2
MTLE (*vc*)	8.7	8.3	8.3

In fact, for instance, the variation of time T_1 from its minimum, calculated with the MTLL model at $\phi = 0°$, and its maximum, calculated at $\phi = 180°$, is of about 27%, independently from the distance d. Such a variation can be explained if we consider that at $\phi = 0°$ the lightning channel is inclined towards the observer, while the observer at $\phi = 180°$ sees the channel leaning away. This behavior could also explain the discrepancy between simulated and measured data that do not take into account the variation from the vertical position of the lightning channel. The changes of the zero-crossing time in the MTLE model are less pronounced (about 20%), although still evident, due to the exponential decay of return stroke current amplitude.

As concerns as the opposite polarity overshoot described by the ratio E_p/E_o, it has its maximum at $\phi = 0°$ and its minimum on the opposite observation point $\phi = 180°$. The variation is about 15% and, again, it is probably due to the weaker effect of the return stroke current when it flows along a channel that is pending away from the observation point with respect to a current flowing in channel that is inclined towards the observer.

4.5. Effect of Channel Tortuosity

The effect of channel tortuosity has been schematically studied by considering a slanted channel composed of 8 segments (Figure 4(c)). The plot of the vertical electric field waveforms calculated with $\beta = 0.3$ at 75 km is shown in Figure 9 for the four different observation points and for both MTLL (Figure 9(a)) and MTLE (Figure 9(b)) models. In such a plot the time scale has been changed and only the first 100 µs are shown in order to put in evidence the different characteristics of fields. Moreover, for comparison, the plot of the electric field for a vertical channel vc has also been added.

Interesting features appear since the effect of tortuosity is given by significant "humps" in the waveforms visible at position $\phi = 0°$ and $\phi = 180°$ because a change of channel inclination is reflected in attenuation or amplification of the electric field. In contrast, at positions $\phi = +90°$ and $\phi = -90°$ the electric field has a regular shape with no visible jaggedness, since the channel lays only in the xz-plane.

Since tortuosity has effect on the fine structure of electric fields, it also affects its frequency content, which sensibly increases if compared to vertical channels [31]. In fact, at each kink, there is a change in the direction of propagation of the current which introduces a rapid change in the electric field. Obviously, the reproduced fields depicted in Figure 9 have a regular shape since a regular slanted channel has been adopted, but it is possible to state that the adoption of a real tortuous lightning path could lead to field waveforms similar to the one reproduced in Figure 1. Work is in progress in order to collect 3-d data of real lightning channels and reproduce with accuracy the generated fields.

Furthermore, tortuosity does not significantly affect the parameters T_1 and T_R which remain practically unchanged, while it has some influence on only one parameter characterizing distant fields,

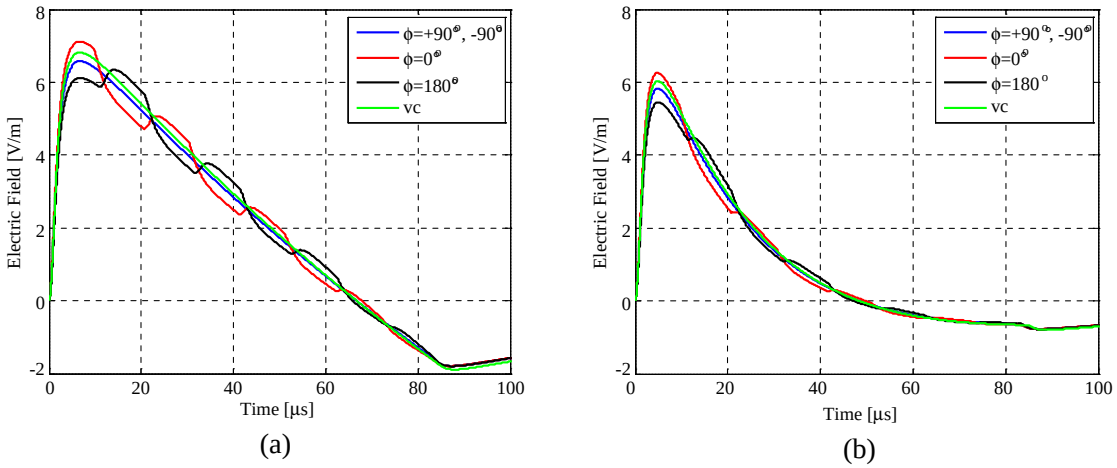

Figure 9. Electric field at ground for the slanted channel (sc_8) and $\beta = 0.3$, MTLL (Figure 9(a)) and MTLE (Figure 9(b)). Effect of observer position P.

that is the ratio E_p/E_o which can increase of about 15% depending on the observation point. Complete data are reported in Table 5 in which the values of the ratio E_p/E_o obtained for the slanted channel sc_8 in all observation points are compared with the same parameter calculated for a vertical channel sc. The variation of E_p/E_o with channel inclination, tortuosity and distance could be a possible explanation of the differences in this parameter between results of simulations and experimental data, although it cannot fully take into account the strong decrease (about 50%) of E_p/E_o when moving from 50 km to 250 km away from the channel base.

5. CONCLUSIONS

In the present paper a numerical investigation on distant electric fields produced by lightning return strokes has been carried out in order to examine different factors influencing the field waveforms at distances above 50 km. Results have been compared to experimental data found in the updated literature. The *OPO* duration T_2 cannot be reproduced because the in-cloud portion of the channel and the ionospheric reflection are not considered in the MTLL and MTLE models. The Opposite Polarity Overshoot, the zero-crossing time and the zero-to-peak risetime, characteristics of distant fields, depend not only on the return stroke speed and on the distance from the lightning source but also on the lightning channel geometry and, in particular, on its inclination with respect to ground and on its tortuosity. Such aspects should be taken into account and not neglected in computer models used for the estimation of EM fields generated by lightning.

REFERENCES

1. Uman, M. A. and V. A. Rakov, *Lightning Physics and Effects,* Cambridge University Press, 2003.
2. Borghetti, A., A. S. Morched, F. Napolitano, C. A. Nucci, and M. Paolone, "Lightning-induced overvoltages transferred through distribution power transformers," *IEEE Trans. Power Del.*, Vol. 24, No. 1, 360–372, Jan. 2009.
3. Uman, M. A., *The Art and Science of Lightning Protection,* Cambridge University Press, New York, 2008.
4. Andreotti, A., C. Petrarca, V. A. Rakov, and L. Verolino, "Calculation of voltages induced on overhead conductors by nonvertical lightning channels," *IEEE Trans. on Electromagn. Compat.*, Vol. 54, No. 4, 860–870, Jan. 2012.
5. Noda, T., M. Sakae, and S. Yokoyama, "Simulation of lightning surge propagation from distribution line to consumer entrance via pole-mounted transformer," *IEEE Trans. on Power Delivery*, Vol. 19, No. 1, 442–444, 2004.
6. De Vivo, B., P. Lamberti, V. Tucci, and C. Petrarca, "Simulation of the bearing voltage in an inverter-fed induction motor by a full three phase multi conductor," *Progress In Electromagnetics Research B*, Vol. 46, 233–250, 2013.
7. Rakov, V. A. and M. A. Uman, "Review and evaluation lightning return stroke models including some aspects of their application," *IEEE Trans. on Electromagn. Compat.*, Vol. 40, No. 4, 403–426, 1998.
8. Rakov, V. A. and F. Rachidi, "Overview of recent progress in lightning research and lightning protection," *IEEE Trans. on Electromagn. Compat.*, Vol. 51, No. 3, 428–442, 2009.
9. Lin, Y. T., M. A. Uman, J. A. Tiller, R. D. Brantley, W. H. Beasley, E. P. Krider, and C. D. Weidman "Characterization of lightning return stroke electric and magnetic fields from simultaneous two-station measurements," *J. Geophysical Research*, Vol. 84, 6307–6314, 1979.
10. Shoory, A., F. Rachidi, M. Rubinstein, R. Moini, and S. H. H. Sadeghi, "Analytical expression for zero-crossing times in lightning return-stroke engineering models," *IEEE Trans. on Electromagn. Compat.*, Vol. 51, No. 4, 963–974, 2009.
11. Shoory, A., F. Rachidi, M. Rubinstein, R. Moini, and S. H. H. Sadeghi, "Why do some lightning return stroke models not reproduce the far-field zero crossing?," *J. Geophysical Research*, Vol. 114, D16204, 2009.

12. Lupò, G., C. Petrarca, V. Tucci, and M. Vitelli, "EM fields associated with lightning channels: On the effect of tortuosity and branching," *IEEE Trans. Electromagn. Compat.*, Vol. 42, No. 4, 394–404, Nov. 2000.
13. Andreotti, A., U. De Martinis, C. Petrarca, V. A. Rakov, and L. Verolino, "Lightning electromagnetic fields and induced voltages: Influence of channel tortuosity," *30th URSI General Assembly and Scientific Symposium, URSIGASS*, Paper 6050702, Turkey, 2011.
14. Pavlick, A., D. E. Crawford, and V. A. Rakov, "Characteristics of Distant lightning electric fields," *Proc. of Intl. Conf. on Probabilistic Methods Applied to Power Systems (PMAPS)*, 703–707, Naples, Italy, Sep. 22–26, 2002.
15. Haddad, M. A. and V. A. Rakov, "New measurements of distant lightning electric fields in Florida: Waveform characteristics, interaction with the ionosphere, and peak current estimates," *J. Geophysical Research*, Vol. 117, D10101, 2012.
16. Haddad, M. A., V. A. Rakov, and S. A. Cummer, "New measurements of lightning electric fields in Florida: Waveform characteristics, interaction with the ionosphere, and peak current estimates," *J. Geophysical Research*, Vol. 117, D110101, 2012.
17. Lupò, G., C. Petrarca, V. Tucci, and M. Vitelli, "EM fields generated by lightning channels with arbitrary location and slope," *IEEE Trans. on Electromagn. Compat.*, Vol. 42, No. 1, 39–53, Feb. 2000.
18. Andreotti, A., G. Lupò, and C. Petrarca, "Evaluation of EM fields from return stroke for indirect — Lightning protection of wind turbines," *2013 International Conference on Clean Electrical Power (ICCEP)*, 755–759, Alghero, Italy, Jun. 2013.
19. Ogata, K., *Modern Control Engineering,* Prentice Hall, New York, 1976.
20. Rachidi, F., W. Janischewskyj, A. M. Hussein, C. A. Nucci, S. Guerrieri, B. Kordi, and J.-S. Chang, "Current and electromagnetic field associated with lightning-return strokes to tall towers," *IEEE Trans. on Electromagn. Compat.*, Vol. 43, No. 3, 39–53, 2001.
21. Uman, M. and D. K. McLain, "Magnetic field of the lightning return stroke," *J. Geophysical Research*, Vol. 74, 6899–6910, 1969.
22. Rakov, V. A. and A. A. Dulzon, "A modified transmission line model for lightning return stroke field calculations," *9th Int. Symposium on Electromagn. Compat.*, 229–235, Zurich, Switzerland, Mar. 1991.
23. Nucci, C. A., C. Mazzetti, F. Rachidi, and M. Ianoz, "On lightning return stroke models for LEMP calculations," *19th International Conference on Lightning Protection (ICLP)*, Graz, Austria, Apr. 1988.
24. Bruce, C. E. R. and R. H. Golde, "The lightning discharge," *J. Inst. Electr. Eng.*, Vol. 88, 487–520, 1941.
25. Heidler, F., "Lightning electromagnetic pulse, theorie und messungen," Ph.D. Dissertation, Fakultät der Elektrotechnik, Univ. Bundeswehr, Munich, Germany, 1987.
26. Diendorfer, G. and M. A. Uman, "An improved return stroke model with specified channel-base current," *J. Geophysical Research*, Vol. 95, 13621–13644, 1990.
27. Uman, M., D. K. McLain, and E. P. Krider, "The electromagnetic radiation from a finite antenna," *Am. Journal of Physics*, Vol. 43, 33–38, 1975.
28. Idone, V. P. and R. E. Orville, "Lightning return stroke velocities in the Thunderstorm Research International Program (TRIP)," *Journal of Geophysical Research Letters*, Vol. 87, No. C7, 4903–4916, Jun. 1982.
29. Hill, R. D., "Analysis of irregular paths of lighting channels," *J. Geophysical Research*, Vol. 73, No. 6, 1897–1906, 1968.
30. Uman, M., J. Schoene, V. Rakov, K. J. Rambo, and G. H. Schnetzer, "Correlated time derivatives of current, electric field intensity and magnetic flux density for triggered lightning at 15 m," *J. Geophysical Research*, Vol. 107, 4160–4172, 2002.
31. LeVine, D. M. and R. Meneghini, "Simulation of radiation from lightning return strokes: The effects of tortuosity," *Radio Sci.*, Vol. 13, No. 5, 801–809, Sep./Oct. 1978.